Published in final edited form as:

Acta Biomater. 2013 July ; 9(7): 7420–7428. doi:10.1016/j.actbio.2013.04.005.

Maximizing phenotype constraint and extracellular matrix production in primary human chondrocytes using arginine–glycine–aspartate concentration gradient hydrogels

Laura A. Smith Callahan[a], **Erin P. Childers**[a], **Sharon L. Bernard**[a], **Scott D. Weiner**[b], and **Matthew L. Becker**[a,c,*]

[a]Department of Polymer Science, The University of Akron, Akron, OH 44325, USA

[b]Department of Orthopedic Surgery, Summa Health Systems, Akron, OH 44325, USA

[c]Center for Biomaterials in Medicine, Austen Bioinnovation Institute in Akron, Akron, OH 44308, USA

Abstract

New systematic approaches are necessary to determine and optimize the chemical and mechanical scaffold properties for hyaline cartilage generation using the limited cell numbers obtained from primary human sources. Peptide functionalized hydrogels possessing continuous variations in physico-chemical properties are an efficient three-dimensional platform for studying several properties simultaneously. Herein, we describe a polyethylene glycol dimethacrylate (PEGDM) hydrogel system possessing a gradient of arginine–glycine–aspartic acid peptide (RGD) concentrations from 0 mM to 10 mM. The system is used to correlate primary human osteoarthritic chondrocyte proliferation, phenotype maintenance and extracellular matrix (ECM) production to the gradient hydrogel properties. Cell number and chondrogenic phenotype (CD14:CD90 ratios) were found to decline in regions with higher RGD concentrations, while regions with lower RGD concentrations maintained cell number and phenotype. Over three weeks of culture, hydrogel regions containing lower RGD concentrations experience an increase in ECM content compared to regions with higher RGD concentrations. Variations in actin amounts and vinculin organization were observed within the RGD concentration gradients that contribute to the differences in chondrogenic phenotype maintenance and ECM expression.

Keywords

Cartilage; Tissue engineering; Hydrogel; Combinatorial methods; Gradient

1. Introduction

The incidence of cartilage injury during both athletic and normal activities is substantial, as is the cost of treating these injuries [1–4]. Complicating the recovery process is the fact that unlike bone, cartilage generally has a limited capacity to repair itself [5]. The aggregate

*Corresponding authors. Address: Department of Polymer Science, The University of Akron, Goodyear Polymer Center #517, Akron, OH 44325-3909, USA. Tel.: +1 330 972 2834; fax: +1 330 972 5290., becker@uakron.edu (M.L. Becker).

expenditures for the treatment of osteoarthritis (OA) is expected to increase to US$185.5 billion per year (in 2007 US dollars) [6] over the next decade. The Osteoarthritis Research Society International Disease State Working Group with the US Food and Drug Administration has determined that future treatments should focus on preserving the joint and addressing the underlying mechanical changes in cartilage during the progression of OA [7]. Upon degeneration associated with damage of the extracellular matrix (ECM), osteoarthritis develops and, depending on the progression, requires a surgical intervention to alleviate patient pain and discomfort. While many surgical options exist including microfracture and debridement, they are designed to be palliative rather than restorative since they do not lead to the regrowth of hyaline cartilage.

One of the most significant barriers to restorative tissue engineering approaches is the limitation associated with cell sourcing and safety. While many groups are pursuing modified progenitor and mesenchymal stem cell approaches with great fanfare and results, the hurdle for safety associated with stem cell technology is much higher for orthopedic repairs compared to other life-threatening cardiovascular events where stem cells have shown great clinical efficacy [8,9]. In the near term, the translationally relevant source remains autologous cells. Autologous chondrocyte implantation (ACI) has been used safely albeit with inconsistent results for more than two decades. ACI is described in numerous papers [10–13] and involves two separate surgical procedures, with the first being a cartilage harvesting biopsy after which the isolated chondrocytes are expanded for a few weeks ex vivo. The second operation includes an arthrotomy, preparation or trimming of the defect site, fixation of harvested periosteal tissue (from the donor) over the defect, securing a watertight seal with fibrin glue and injecting the chondrocyte suspension [11]. There is no preorganization of the cells in a scaffold prior to implantation. The cells are typically cultured in Dulbecco’s modified Eagle medium/F-12 1:1 supplemented with 10% of the autologous serum, gentamicin sulfate, amphotericin B, L-ascorbic acid and L-glutamine [10,14]. When reimplanted they are suspended in Ham’s F-12 medium containing 20% autologous serum [14]. A more biomimetic, scaffold-based tissue engineering approach is likely needed to enhance restorative potential to future patients. Tissue engineering has the potential to extend joint life and provide mechanical support for the generation of biomimetic hyaline cartilage. However, ideal scaffold materials and conditions to generate ex vivo or regenerate in situ tissues possessing native structure and properties have yet to be determined and likely differ for various populations. One strategy to achieve regeneration is to emulate aspects of the native extracellular matrix (ECM). In tissues like cartilage where the chondrocyte function is significantly influenced by ECM interactions [15], scaffolds presenting ECM-mimicking signals can be particularly useful.

Cartilage oligomeric matrix protein (COMP), a protein found in cartilage thought to play a role in organizing the cartilage ECM [16–18], has been shown to bind to chondrocytes utilizing an arginine–glycine–aspartate (RGD) tripeptide sequence and a α5-integrin receptor [19]. In addition, COMP binds and co-localizes with fibronectin, another RGD containing protein important in early cartilage development, on the surface of human chondrocytes [16]. This indicates that both proteins may provide signaling to the chondrocytes. The RGD tripeptide sequence is found in many ECM proteins and promotes cellular adhesion through interaction with many integrins [20,21]. On numerous

biomaterials, RGD increases cellular adhesion and alters cellular behavior [22–25]. Previous studies utilizing biomaterials are inconclusive as to whether RGD is beneficial to chondrocyte culture and cartilage formation [26–31]. We postulate that differences in concentration and bioavailability contribute to the wide variation in results. To examine this, combinatorial methods, which are used in the pharmaceutical industry and recently adapted for use in biomaterials and tissue engineering [32,33], are utilized.

However, many combinatorial methods are designed for two-dimensional (2-D) screening applications instead of three-dimensional (3-D) ones, which more closely replicate native tissue [34]. A continuous hydrogel gradient strategy maximizes the number of material conditions examined and has been adapted for 3-D tissue engineering [35–37]. As such, a continuous gradient strategy is utilized to systematically screen the effect of RGD concentration on human chondrocyte function. Herein, we describe a facile method to fabricate polyethylene glycol dimethacrylate (PEGDM) hydrogels possessing a concentration profile of RGD that is defined spatially. We assess the fidelity of our fabrication methods by characterizing the RGD content and bioavailability using multiple methods. The well-defined samples are then used to examine the effect of RGD concentration on cellular proliferation, phenotype maintenance, cytoskeletal organization and the secretion of ECM from primary human chondrocytes isolated from OA cartilage.

2. Experimental methods

2.1. Cell isolation

Institutional Review Board (IRB) approval was obtained at each of the institutions involved for use of human tissue. Chondrocytes were isolated from the tibial plateaus and femoral condyles of patients undergoing total knee arthoplasty (average age: 51.5 years, range: 46–55 years, total knees (female): 8(6)). Isolated tissue was placed in 4 mg ml^{-1} collagenase in Hank's buffered salt solution for at least 4 h and washed twice with phosphate buffered saline (PBS; Invitrogen, Carlsbad, CA). Cell suspension was then passed through a 22 mm diameter ~80 μm stainless steel syringe filter to remove cellular debris and encapsulated in hydrogels immediately after isolation.

2.2. RGD synthesis

GRGDS (RGD) was synthesized using standard solid-phase FMOC chemistry on Wang's resin or purchased from American Peptide (Sunnyvale, CA). A photopolymerizable acrylate group was coupled to the N-terminus of each peptide during synthesis. Peptides were cleaved from the resin using standard conditions (45 m, 95% trifluoroacetic acid, 2.5% triisopropylsilane, 2.5% water (all vol.%)) and precipitated in diethyl ether. Following two trituration cycles, the peptides were dialyzed in deionized water (molecular mass (MW) cutoff 100–500 Da, cellulose ester, Spectrum, Rancho Domingo, CA), and the formal weight was verified with matrix-assisted laser desorption ionization-time of flight (MALDITOF) (FW:acrylic acid-GRGDS = 545.3 g mol^{-1}).

2.3. Hydrogel fabrication

11.5% PEGDM (~8000 g mol^{-1}) (Monomer-Polymer & Dajac Labs, Trevose, PA) solutions in Opti-MEM with or without 15 mM RGD were prepared containing 0.1% Irgacure 2959 (Ciba Specialty Chemicals, Basel, Switzerland). Solutions were loaded into 1 m syringes and placed in a computer driven syringe pump system (Fig. 1A and B) to create RGD-gradient hydrogels (Fig. 1C). Computer controlled syringe pumps were used to dispense 11.5% PEGDM solutions with and without 15 mM RGD in inverse ramping profiles ranging from 53 ml h^{-1} to 0 ml h^{-1} over 90 s into a custom mold while 11.5% PEGDM solution without RGD was dispensed at a constant rate of 10 ml h^{-1} (Fig. 1D). The mold possessed a depth profile (1 mm) to minimize diffusional mixing during gradient formation. Hydrogels were photopolymerized using ~2.3 mJ cm^{-2} UVA light for 5 min and then placed in Opti-MEM I reduced-serum medium for storage. Unless otherwise noted, all samples for analysis were 5 mm by 10 mm by 1 mm. For cellular experiments, 11.5% PEGDM solution without RGD dispensed at a constant rate contained 3.85×10^6 cells ml^{-1} leading to a final cell content of 778,000 cells per gradient. Cellular samples were cultured up to 3 weeks in Opti-MEM I reduced-serum medium containing 50 μgml^{-1} ascorbate and 100 μgml^{-1} primocin at 37 °C in a 5% CO_2 incubator. Media were changed every other day.

2.4. Hydrogel characterization

For swelling studies, samples were weighed and measured immediately after photopolymerization and were then placed in Opti-MEM at 37 °C in a 5% CO_2 incubator for 24 h. Following incubation, the samples were blotted dry before being weighed and measured again. The samples were then placed in a freeze dryer and thoroughly dried before being weighed again. Swelling ratio, q, was determined by taking the ratio of the swollen mass of the hydrogel by the mass of the hydrogel after freeze drying. The mesh size was determined as described by Canal and Peppas [38] using the equation $\xi = V_{2,s}^{-1/3} l C_n^{1/2} n^{1/2}$ with the alteration proposed by Anseth [39] and Hubbel [40]. $V_{2,s}$ is the equilibrium polymer volume fraction in the gel, l is the bond length (1.50 Å) [40], C_n is the characteristic ratio of PEG [41], and n is the number of bonds between crosslinks.

To determine the storage modulus, 8 mm diameter samples were punched from gradients every 10 mm with a gasket punch and tested on an ARES-G2 rheometer (TA Instruments, Newcastle, DE) using 8 mm serrated parallel plates with a strain amplitude of 1% and 30 N constant normal force to prevent slippage over an angular frequency sweep from 100 to 1 rad s^{-1} with 10 points per decade. Modulus data are reported at an angular frequency of 1 rad s^{-1} since gels did not show a frequency-dependent response. Young's and shear modulus were measured on 5 mm gradient sections using a TA.XTplus Texture Analyser (Stable Micro Systems, Surrey, UK) with a ¼ in. spherical probe. The probe penetrated the gels at a constant velocity of 0.01 mm s^{-1}. Force (N), depth (mm), time (s) and strain data were collected. The contact radius (Eq. (1)) [42], indentation stress (Eq. (2)) [42], Young's modulus (Eq. (3)) [42] and shear modulus (Eq. (4)) [43] were calculated using the following equations:

$$a = R^{1/2} \delta^{3/2} \quad (1)$$

$$\sigma = F/(\pi a^2) \quad (2)$$

$$E = \sigma 3\pi(1-\upsilon)/(20\varepsilon) \quad (3)$$

$$\begin{aligned} G &= 3P_i/(16afp((\sqrt{R\delta})/h)) \text{ and } fp((\sqrt{R\delta})/h)) \\ &= ((\sqrt{R\delta})/h)^2 + 0.82((\sqrt{R\delta})/h) + 0.46/(((\sqrt{R\delta})/h) + 0.46) \end{aligned} \quad (4)$$

where R is the radius of indentor, δ is depth of indentions, F is applied force, υ is Poisson's ratio of polyethylene glycol, ε is strain, P_i is the load response and h is the height of the hydrogel.

RGD peptide content in the gradient hydrogels was accessed using a Lowry assay [44]. Gradients were placed in ultrapure water for 3 days on an orbital shaker at 50 rpm. The water was changed every day. Gradients were then placed in Reagent B (Dc Protein assay (Biorad, Hercules, CA) on the orbital shaker for 30 min, after which they were placed in Reagent A for 30 min. Gradients were washed in ultrapure water and a circular sample was taken every 10 mm down the length of the gradient. The absorbance at 750 nm was read from each gradient sample and compared to the absorbance of hydrogel samples of known RGD content for normalization. The bioavailability of RGD was determined in a manner similar to one previously described using a peptide designed to mimic the natural integrin receptor (CWDDGWLC-biotin) (American Peptide, Sunnyvale, CA) and Alexaflour 488 streptavidin colloidal gold (Invitrogen) [45]. Briefly, samples were blocked for 1 h with bovine serum albumin in RGD blocking buffer, washed for 5 min in RGD wash buffer five times and incubated overnight at ambient temperature on an orbital shaker at ~75 rpm in 0.1 mg ml^{-1} integrin mimicking peptide in RGD wash buffer. Samples were washed five more times for 5 min each in RGD wash buffer to remove unbound peptide and incubated in 3 ng ml^{-1} Alexaflour 488 streptavidin colloidal gold nanoparticle solution overnight at ambient temperature on an orbital shaker at ~75 rpm. Samples were washed five times for 5 min each in RGD wash buffer to remove unbound Alexaflour 488 streptavidin colloidal gold and then viewed on an IX81 microscope (Olympus, Center Valley, PA).

2.5. Histological staining and immunohistochemistry

All samples were fixed overnight in 4% paraformaldehyde (Sigma). Whole mount histological staining samples were transferred to PBS and stained with 0.5% Alcian blue (Sigma) for 3 h at room temperature. Samples were then washed with PBS and water and imaged on a CKX41 microscope (Olympus). Whole mount samples for CD14 (SC9150, Santa Cruz, 1:100) and CD90 (SC6071, Santa Cruz, 1:100) were washed in PBS thrice for 5 min each and once in 0.1% donkey serum with 0.01% sodium azide in PBS for 30 min at room temperature. Donkey serum (10%) was used to block for 1 h. Samples were incubated in primary antibodies overnight then stained with appropriate Alexaflour secondary antibodies and DAPI for 1 h, washed and then viewed. Image J (National Institute of Health, Bethesda, MD, http://rsb.info.nih.gov/ij/) was used to determine the frequency of CD14 and CD90 in the cell population for at least 90 cells from three separate gradients at each

position. The fraction of cells in the total cell population expressing CD14 and CD90 was determined. The CD14/CD90 ratio was obtained by then dividing the fraction of cells in the total population expressing CD14 by the faction of cells in the total cell population expressing CD90. These values were then normalized to the day 10, 45 mm gradient position. Images were not adjusted or thresholded.

Whole mount cytoskeletal staining samples were transferred to 0.5% Triton x-100 in cytoskeleton stabilization (CS) buffer (0.1 M PIPES, 1 mM EGTA, and 4% (w/v) 8000MW polyethylene glycol) at 37 °C for 10 min, rinsed thrice for 5 min each in CS buffer and incubated in 0.05% sodium borohydride in PBS at ambient temperature for 10 min. Whole mount samples were then blocked in 5% donkey serum for 20 min at 37 °C and incubated overnight at 4 °C with vinculin antibody (V4505, Sigma, 1:100) and rhodamine phalloidin (1:200). Samples were then washed thrice with 1% donkey serum for 5 min, followed by appropriate secondary antibodies conjugated to FITC. DAPI was used to stain the cell nuclei. Cellular area and number of vinculin adhesion sites were quantified with the automated measurement and counting features of Image J for at least 60 cells from four separate gradients at each position. Samples for histological sectioning were transferred to 70% ETOH for at least 1 h, 80% ETOH for 1.5 h, 95% ETOH for 12 h, ETOH for 1.5 h twice and xylene for 1 h. Samples were then placed in a 60 °C paraffin bath for 12 h and embedded in a paraffin block for sectioning [46]. Blocks were removed from a −20 °C freezer and cut into 7 μm sections. After 2 days of drying in a 37 °C oven, samples were stained with picro-sirius red solution with Mayer's haematoxylin (Fisher Biological, Pittsburgh, PA) after paraffin removal with xylene and rehydration through an ethanol gradient. After rehydration, immunochemistry samples were incubated in 0.5% pepsin for 10 min at 30 °C for antigen retrieval. Nonspecific antibody binding was blocked by incubating in 10% goat serum, then samples were exposed to collagen type 2 (1:200) antibody, followed by appropriate secondary antibodies (Col 2) conjugated to FITC. DAPI was used to stain the cell nuclei. The Col 2 antibody (IIII6B3) developed by Thomas F. Linsenmayer was obtained from the Developmental Studies Hybridoma Bank developed under the auspices of the NICHD and maintained by The University of Iowa, Department of Biology. Col 1A antibody (sc-25974) was obtained from Santa Cruz Biotechnology (Santa Cruz, CA) and DAPI was obtained from Sigma.

2.6. Biochemistry

Samples were homogenized with a Tissue-Tearor (BioSpec Products, Inc., Bartlesville, Oklahoma). DNA content was determined with a fluorescence assay from Sigma according to the manufacturer's protocol. Sulfated glycosaminoglycans (sGAGs) were quantified with dimethylmethylene blue (DMB), while collagen content was quantified using dimethylaminobenzaldehyde (DAB) to observe chloramines T-oxidized hydroxyproline as previously described [47–50]. Briefly, samples were homogenized and were then digested with proteinase K overnight at 60 °C. Samples for sGAGs detection were added to DMB solution at a ratio of 1:10, mixed and read at 535 nm. Samples for hydroxyproline detection were dehydrated, autoclaved at 120 °C with 2 N NaOH for 20 min, oxidized with chloramines T solution for 25 min at room temperature on an orbital shaker at 100 rpm and then incubated with DAB for 20 min at 65 °C. The absorbance is then read at 550 nm.

2.7. Statistics

All experiments were conducted at least three times ($n \geq 3$). All quantitative data are presented as the average ± standard deviation. One-way analysis of variance (ANOVA) with Tukey post hoc analysis (comparisons of more than two groups) or a *T* test (two group comparisons) were performed where applicable. Significance was set at a *P*-value of less than 0.05.

3. Results

The mechanical properties of the RGD gradient hydrogels did not vary significantly throughout the gradient (Fig. 2A). The Lowry and receptor mimic nanoparticle assays were used to show that the concentration of RGD was controllably varied from ~0mM to 10 mM (Fig. 2B and C), indicating that a functional RGD gradient was fabricated. Over the course of 10 days of culture, fewer chondrocytes cultured in gradients with higher RGD concentration levels survived compared to chondrocytes cultured in gradients containing the lower RGD concentrations (Fig. 3A). At the highest RGD concentration, reduced survival was evident after 5 days of culture, while significant cellular loss was not evident until 10 days of culture in other RGD concentration regions. In addition, the ratio of surface marker CD14 (a lipopolysaccharide receptor found on freshly isolated chondrocytes [51,52]) expression to that of surface marker CD90 (a glycosylphosphatidylinositol-anchored glycoprotein associated with cellular proliferation [51,53], which is present in low amounts on freshly isolated chondrocytes [52]) expression was used to quantify chondrocyte phenotype maintenance [51,54–56] since the CD14/CD90 ratio decreases more rapidly with time (10,000-fold after one passage at the protein level and 1000-fold after 10 days at the mRNA level) than traditional phenotype indicators, such as the Col 2:Col 1 (ten-fold after 10 days at the mRNA level) and aggrecan:versican (fivefold after 10 days at the mRNA level) ratios [54,55]. Chondrocytes cultured in gradients with lower RGD concentrations maintained the chondrogenic phenotype relative to the chondrocytes in the highest levels of RGD concentrations after 2 days of culture (Fig. 3B). Intermediate RGD concentrations experienced phenotype loss over time, indicating that lower RGD levels promote maintenance of phenotype relative to higher RGD concentrations.

RGD concentrations have been shown to influence chondrocyte shape [26,57], which can modulate focal contact adhesions and cytoskeletal arrangement, thereby altering cellular behavior [58,59]. As such, actin and vinculin organization were observed in our system over 10 days of culture (Fig. 4). After 2 days of culture, chondrocytes in the gradient region with lower RGD concentrations were less spread than chondrocytes in regions with higher RGD concentrations (Fig. 4C). However, after 10 days of culture, chondrocytes in the lowest RGD regions increased their cell area while chondrocytes in the other concentration regions reduced their cellular area. The number of vinculin adhesion after 2 days of culture was significantly higher in chondrocytes encapsulated in regions with lower RGD content compared to chondrocytes in gradient regions with higher RGD content (Fig. 4D). As culture continued, the number of vinculin adhesion sites increased at every gradient position (Fig. 4D).

Since changes in cytoskeletal arrangement can alter ECM synthesis [60–62], the ECM content in gradient regions was examined after 3 weeks of culture (Fig. 5). Lower RGD content regions contained more sGAGs (Fig. 5A and D) and collagen (Fig. 5B, C and E) than higher RGD content regions. Increased levels of Col 2, the principal collagen in the cartilage ECM, was found in regions with lower RGD content compared to regions with higher RGD content (Fig. 5C).

4. Discussion

The systematic optimization of tissue engineering scaffolds remains a challenge [63]. Many physical and chemical factors play a role in successful tissue formation [24,25,36,47,64]. 3-D hydrogel gradients represent a straightforward way to systematically examine the modulation of many factors for tissue formation to determine optimal scaffold characteristics. For this strategy to be successful, the gradients and scaffolds must be precisely characterized. However, the bioavailable concentration of tethered bioactive peptides is rarely examined within the finished scaffolds even though scaffold processing has been shown to affect the bioavailable concentration of factors [45,65]. In this paper we present the bioavailability and characterization of the RGD concentration within our gradients, but also show this concentration gradient to have significant effect human chondrocyte survival, phenotype and ECM synthesis.

Previous studies observed conflicting results of the effects of RGD concentration on mechanical properties of PEG hydrogels [26,66]. Changes in mechanical properties were not observed in our system (Fig. 2A). PEGDM hydrogels with a wide range of mechanical properties (storage modulus from 1000 Pa to 530,000 Pa, swelling ratio from 4 to 35, mesh size from 40 Å to 140 Å, etc.) have been used for cartilage tissue engineering applications [56,67–69]. One recent study utilizing PEGDM hydrogels processing a modulus gradient found that optimal ECM formation and phenotype maintenance occurred when OA human chondrocytes were encapsulated in hydrogels with a storage modulus of ~4500 Pa, a swelling ratio of ~13 and a mesh size of ~116 Å [56], which are all similar to the values reported here. The inconsistencies represented in the literature are most likely due to differences in the respective polymer systems or testing conditions. Both the concentration (Fig. 2B) and bioavailability studies (Fig. 2B and C) indicate the presence of an RGD gradient of known concentration that is well-defined spatially. This additional characterization will allow the gradient system to be adapted quickly into discrete scaffolds with optimized characteristics and for the systematic study of RGD concentrations in biological systems to help elucidate the factors leading to inconsistencies in the literature.

This study suggests that lower RGD content improves chondrocyte survival (Fig. 3A), phenotype maintenance (Fig. 3B) and extracellular matrix synthesis (Fig. 5) compared to high RGD concentrations, which can become toxic to OA human chondrocytes. A previous study with bovine chondrocytes observed that changes in RGD concentration had no effect on proliferation and ECM synthesis, but higher RGD concentrations did decrease phenotype maintenance [26]. Another study by the same group with similar hydrogels observed a decrease in collagen content at intermediate RGD concentrations, but similar collagen synthesis at higher RGD concentrations [31]. Studies by other groups found RGD to

increase collagen deposition over the control [28] and sGAGs synthesis to decrease with increasing RGD content [29]. Differences may be in cell sourcing, since animal sourced chondrocytes may not have a similar response to biomaterials as clinically relevant human chondrocytes [50]; this may contribute to the inconsistency of results between studies. In addition, variations in the bioavailable RGD concentration, polymeric systems and culture conditions could contribute to the variations in results. Discerning the effects of each is not possible from the current literature and this underscores the need for more systematic studies, like this one.

Osteoarthritis progression leads to changes in chondrocyte morphology [15] that have been linked to changes in the pericellular matrix content and thickness [70]. Thus changing chondrocyte ECM interactions and signaling, potentially leading to the phenotype changes associated with changes in chondrocyte cytoskeleton arrangements [71]. Changes in cytoskeletal organization observed in this study (Fig. 4C) are similar to a previous 2-D study. It found that higher RGD concentrations led to an initial increase in chondrocyte spreading followed by a decrease in the chondrocyte foot-print over time and an increase of initial spreading over the control but leads to decreased cell size over time [27]. The organization of actin within chondrocytes is also thought to contribute to cellular phenotype, pericellular matrix synthesis and retention of the proteoglycans in the tissue [62,72]. This may contribute to phenotype and ECM synthesis difference observed in chondrocytes at the lowest RGD concentrations. The actin organization tends to be more localized toward one side of the cell (Fig. 4A and B), reminiscent of the apical organization of actin in healthy chondrocytes [73]. While chondrocytes in regions with increased RGD concentrations show cytoskeletal organization that appears less organized cortically (Fig. 4A and B), similar to previous reports of OA chondrocytes [73].

Reduced vinculin signaling has been linked to reduced ECM synthesis and chondrogenic gene expression [74] and may contribute to the ECM synthesis differences observed in this study since chondrocytes in regions with lower RGD concentration had more adhesion sites than chondrocytes in regions with higher RGD concentrations after 2 days of culture (Fig. 4D). As adhesions sites continued to mature, vinculin adhesions increased at all gradient positions as culture time increased.

5. Conclusions

This work presents the development and characterization of a gradient hydrogel system for the systematic study of RGD concentration changes on OA human chondrocyte proliferation, phenotype maintenance and ECM production. Over 10 days of culture, chondrocytes in regions with higher RGD concentrations experience a decline in cell number and chondrogenic phenotype while chondrocytes in gradient regions with lower RGD concentrations maintained cell number and phenotype. Over three weeks of culture, gradient regions with lower RGD concentration experience an increase in ECM content compared to gradient regions with higher RGD concentrations. Variations in actin and vinculin amounts and organization where observed within the RGD concentration gradient could contribute to the differences in chondrogenic phenotype maintenance and ECM expression. Overall, our data indicate that lower RGD concentrations in tissue engineering

scaffolds will better stimulate the potential of OA chondrocytes to secrete more ECM to repair defects and potentially improve integration in ACI procedures. These data are critical in that improving the activation and proliferative activity of autologously harvested cells while maintaining phenotype is a necessary step to efficiently utilize OA chondrocytes as a viable cell source for tissue engineering.

Acknowledgments

The authors gratefully acknowledge research funding from the Akron Functional Materials Center and RESBIO "Integrated Technology Resource for Polymeric Biomaterials" (NIH-NIBIB & NCMHD P41EB001046) which enabled this work. The authors would also like the thank Leann Speering of Summa Health Systems for overseeing IRB approval and arranging tissue transfers.

References

1. Lindahl A, Brittberg M, Peterson L. Health economics benefits following autologous chondrocyte transplantation for patients with focal chondral lesions of the knee. Knee Surg Sports Traumatol Arthrosc. 2001; 9:358–63. [PubMed: 11734874]
2. Aroen A, Loken S, Heir S, Alvik E, Ekeland A, Granlund OG, et al. Articular cartilage lesions in 993 consecutive knee arthroscopies. Am J Sports Med. 2004; 32:211–5. [PubMed: 14754746]
3. Widuchowski W, Widuchowski J, Trzaska T. Articular cartilage defects: study of 25,124 knee arthroscopies. Knee. 2007; 14:177–82. [PubMed: 17428666]
4. Hjelle K, Solheim E, Strand T, Muri R, et al. Articular cartilage defects in 1,000 knee arthroscopies. Arthroscopy. 2002; 18:730–4. [PubMed: 12209430]
5. Hollander AP, Dickinson SC, Kafienah W. Stem cells and cartilage development: complexities of a simple tissue. Stem Cells. 2010; 28:1992–6. [PubMed: 20882533]
6. Kotlarz H, Gunnarsson CL, Fang H, Rizzo JA. Insurer and out-of-pocket costs of osteoarthritis in the US: evidence from national survey data. Arthritis Rheum. 2009; 60:3546–53. [PubMed: 19950287]
7. Lane NE, Brandt K, Hawker G, Peeva E, Schreyer E, Tsuji W, et al. OARSI-FDA initiative: defining the disease state of osteoarthritis. Osteoarthritis Cartilage. 2011; 19:478–82. [PubMed: 21396464]
8. Mathur D, Pereira WC, Anand A. Emergence of chondrogenic progenitor stem cells in transplantation biology—prospects and drawbacks. J Cell Biochem. 2012; 113:397–403. [PubMed: 21928321]
9. Madry H, Cucchiarini M. Clinical potential and challenges of using genetically modified cells for articular cartilage repair. Croat Med J. 2011; 52:245–61. [PubMed: 21674822]
10. Brittberg M, Lindahl A, Nilsson A, Ohlsson C, Isaksson O, Peterson L. Treatment of deep cartilage defects in the knee with autologous chondrocyte transplantation. N Engl J Med. 1994; 331:889–95. [PubMed: 8078550]
11. Batty L, Dance S, Bajaj S, Cole BJ. Autologous chondrocyte implantation: an overview of technique and outcomes. ANZ J Surg. 2011; 81:18–25. [PubMed: 21299794]
12. Minas T, Peterson L. Advanced techniques in autologous chondrocyte transplantation. Clin Sports Med. 1999; 18:13–44. [PubMed: 10028115]
13. Bartlett W, Skinner JA, Gooding CR, Carrington RWJ, Flanagan AM, Briggs TWR, et al. Autologous chondrocyte implantation versus matrix-induced autologous chondrocyte implantation for osteochondral defects of the knee. J Bone Joint Surg-Br. 2005; 87B:640–5. [PubMed: 15855365]
14. Peterson L, Minas T, Brittberg M, Lindahl A. Treatment of osteochondritis dissecans of the knee with autologous chondrocyte transplantation—results at two to ten years. J Bone Joint Surg-Am. 2003; 85A:17–24. [PubMed: 12721341]
15. Scully SP, Lee JW, Ghert MA, Qi W. The role of the extracellular matrix in articular chondrocyte regulation. Clin Orthop Relat Res. 2001:S72–89. [PubMed: 11603727]

16. Di Cesare PE, Chen FS, Moergelin M, Carlson CS, Leslie MP, Perris R, et al. Matrix–matrix interaction of cartilage oligomeric matrix protein and fibronectin. Matrix Biol. 2002; 21:461–70. [PubMed: 12225811]
17. Halász K, Kassner A, Mörgelin M, Heinegård D. COMP acts as a catalyst in collagen fibrillogenesis. J Biol Chem. 2007; 282:31166–73. [PubMed: 17716974]
18. Chen FH, Herndon ME, Patel N, Hecht JT, Tuan RS, Lawler J. Interaction of cartilage oligomeric matrix protein/thrombospondin 5 with aggrecan. J Biol Chem. 2007; 282:24591–8. [PubMed: 17588949]
19. Chen FH, Thomas AO, Hecht JT, Goldring MB, Lawler J. Cartilage oligomeric matrix protein/thrombospondin 5 supports chondrocyte attachment through interaction with integrins. J Biol Chem. 2005; 280:32655–61. [PubMed: 16051604]
20. Ruoslahti E. RGD and other recognition sequences for integrins. Annu Rev Cell Dev Biol. 1996; 12:697–715. [PubMed: 8970741]
21. Dsouza SE, Ginsberg MH, Plow EF. Arginyl-glycyl-aspartic acid (RGD)—a cell-adhesion motif. Trends Biochem Sci. 1991; 16:246–50. [PubMed: 1926332]
22. Hersel U, Dahmen C, Kessler H. RGD modified polymers: biomaterials for stimulated cell adhesion and beyond. Biomaterials. 2003; 24:4385–415. [PubMed: 12922151]
23. Pierschbacher MD, Ruoslahti E. Cell attachment activity of fibronectin can be duplicated by small synthetic fragments of the molecule. Nature. 1984; 309:30–3. [PubMed: 6325925]
24. Acharya AP, Dolgova NV, Moore NM, Xia CQ, Clare-Salzler MJ, Becker ML, et al. The modulation of dendritic cell integrin binding and activation by RGD-peptide density gradient substrates. Biomaterials. 2010; 31:7444–54. [PubMed: 20637504]
25. Moore NM, Lin NJ, Gallant ND, Becker ML. Synergistic enhancement of human bone marrow stromal cell proliferation and osteogenic differentiation on BMP-2-derived and RGD peptide concentration gradients. Acta Biomater. 2011; 7:2091–100. [PubMed: 21272672]
26. Villanueva I, Weigel CA, Bryant SJ. Cell–matrix interactions and dynamic mechanical loading influence chondrocyte gene expression and bioactivity in PEG–RGD hydrogels. Acta Biomater. 2009; 5:2832–46. [PubMed: 19508905]
27. Vonwil D, Schuler M, Barbero A, Strobel S, Wendt D, Textor M, et al. An RGD-restricted substrate interface is sufficient for the adhesion, growth and cartilage forming capacity of human chondrocytes. Eur Cell Mater. 2010; 20:316–28. [PubMed: 21069635]
28. Alsberg E, Anderson KW, Albeiruti A, Rowley JA, Mooney DJ. Engineering growing tissues. Proc Natl Acad Sci. 2002; 99:12025–30. [PubMed: 12218178]
29. Schuh E, Hofmann S, Stok K, Notbohm H, Müller R, Rotter N. Chondrocyte redifferentiation in 3D: the effect of adhesion site density and substrate elasticity. J Biomed Mater Res Part A. 2012; 100A:38–47.
30. Jung HJ, Park K, Kim J-J, Lee JH, Han K-O, Han DK. Effect of RGD-immobilized dual-pore poly(L-lactic acid) scaffolds on chondrocyte proliferation and extracellular matrix production. Artif Organs. 2008; 32:981–9. [PubMed: 19133029]
31. Bryant SJ, Nicodemus GD, Villanueva I. Designing 3D photopolymer hydrogels to regulate biomechanical cues and tissue growth for cartilage tissue engineering. Pharm Res. 2008; 25:2379–86. [PubMed: 18509600]
32. Simon CG, Lin-Gibson S. Combinatorial and high-throughput screening of biomaterials. Adv Mater. 2011; 23:369–87. [PubMed: 20839249]
33. Peters A, Brey DM, Burdick JA. High-throughput and combinatorial technologies for tissue engineering applications. Tissue Eng Part B Rev. 2009; 15:225–39. [PubMed: 19290801]
34. Cukierman E, Pankov R, Stevens DR, Yamada KM. Taking cell–matrix adhesions to the third dimension. Science. 2001; 294:1708–12. [PubMed: 11721053]
35. Tse JR, Engler AJ. Stiffness gradients mimicking in vivo tissue variation regulate mesenchymal stem cell fate. PLoS One. 2011:6.
36. Chatterjee K, Lin-Gibson S, Wallace WE, Parekh SH, Lee YJ, Cicerone MT, et al. The effect of 3D hydrogel scaffold modulus on osteoblast differentiation and mineralization revealed by combinatorial screening. Biomaterials. 2010; 31:5051–62. [PubMed: 20378163]

37. Burdick JA, Khademhosseini A, Langer R. Fabrication of gradient hydrogels using a microfluidics/photopolymerization process. Langmuir. 2004; 20:5153–6. [PubMed: 15986641]
38. Canal T, Peppas NA. Correlation between mesh size and equilibrium degree of swelling of polymeric networks. J Biomed Mater Res. 1989; 23:1183–93. [PubMed: 2808463]
39. Lu S, Anseth KS. Release behavior of high molecular weight solutes from poly(ethylene glycol)-based degradable networks. Macromolecules. 2000; 33:2509–15.
40. Cruise GM, Scharp DS, Hubbell JA. Characterization of permeability and network structure of interfacially photopolymerized poly(ethylene glycol) diacrylate hydrogels. Biomaterials. 1998; 19:1287–94. [PubMed: 9720892]
41. Merrill EW, Dennison KA, Sung C. Partitioning and diffusion of solutes in hydrogels of poly(ethylene oxide). Biomaterials. 1993; 14:1117–26. [PubMed: 8130315]
42. Lin DC, Shreiber DI, Dimitriadis EK, Horkay F. Spherical indentation of soft matter beyond the Hertzian regime: numerical and experimental validation of hyperelastic models. Biomech Model Mechanobiol. 2009; 8:345–58. [PubMed: 18979205]
43. Chan EP, Hu YH, Johnson PM, Suo ZG, Stafford CM. Spherical indentation testing of poroelastic relaxations in thin hydrogel layers. Soft Matter. 2012; 8:1492–8.
44. Miller JS, Shen CJ, Legant WR, Baranski JD, Blakely BL, Chen CS. Bioactive hydrogels made from step-growth derived PEG–peptide macromers. Biomaterials. 2010; 31:3736–43. [PubMed: 20138664]
45. Morgan AW, Roskov KE, Lin-Gibson S, Kaplan DL, Becker ML, Simon CG. Characterization and optimization of RGD-containing silk blends to support osteoblastic differentiation. Biomaterials. 2008; 29:2556–63. [PubMed: 18325585]
46. Strehin, IA.; Elisseeff, JH. Characterizing ECM production by cells encapsulated in hydrogels. In: Even-Ram, S.; Artym, V., editors. Extracellular matrix protocols. New York: Humana Press; 2009. p. 349-62.
47. Smith LA, Liu X, Hu J, Ma PX. The influence of three-dimensional nanofibrous scaffolds on the osteogenic differentiation of embryonic stem cells. Biomaterials. 2009; 30:2516–22. [PubMed: 19176243]
48. Nugent AE, Reiter DA, Fishbein KW, McBurney DL, Murray T, Bartusik D, et al. Characterization of ex vivo-generated bovine and human cartilage by immunohistochemical, biochemical, and magnetic resonance imaging analyses. Tissue Eng Part A. 2010; 16:2183–96. [PubMed: 20136403]
49. Frazier SB, Roodhouse KA, Hourcade DE, Zhang L. The quantification of gycosaminoglycans: a comparison of HPLC, carbazole, and alican blue methods. Open Glycosci. 2008; 1:31–9. [PubMed: 20640171]
50. Callahan LAS, Ganios AM, McBurney DL, Dilisio MF, Weiner SD, Horton WE, et al. ECM production of primary human and bovine chondrocytes in hybrid PEG hydrogels containing type I collagen and hyaluronic acid. Biomacromolecules. 2012; 13:1625–31. [PubMed: 22559049]
51. Diaz-Romero J, Gaillard JP, Grogan SP, Nesic D, Trub T, Mainil-Varlet P. Immunophenotypic analysis of human articular chondrocytes: changes in surface markers associated with cell expansion in monolayer culture. J Cell Physiol. 2005; 202:731–42. [PubMed: 15389573]
52. Summers KL, O'Donnell JL, Hoy MS, Peart M, Dekker J, Rothwell A, et al. Monocyte–macrophage antigen expression on chondrocytes. J Rheumatol. 1995; 22:1326–34. [PubMed: 7562767]
53. Chen X-D, Qian H-Y, Neff L, Satomura K, Horowitz MC. Thy-1 antigen expression by cells in the osteoblast lineage. J Bone Miner Res. 1999; 14:362–75. [PubMed: 10027901]
54. Diaz-Romero J, Nesic D, Grogan SP, Heini P, Mainil-Varlet P. Immunophenotypic changes of human articular chondrocytes during monolayer culture reflect bona fide dedifferentiation rather than amplification of progenitor cells. J Cell Physiol. 2008; 214:75–83. [PubMed: 17559082]
55. Giovannini S, Diaz-Romero J, Aigner T, Mainil-Varlet P, Nesic D. Population doublings and percentage of S100-positive cells as predictors of in vitro chondrogenicity of expanded human articular chondrocytes. J Cell Physiol. 2010; 222:411–20. [PubMed: 19890919]
56. Smith Callahan LA, Ganios AM, Childers EP, Weiner SD, Becker ML. Primary human chondrocyte extracellular matrix formation and phenotype maintenance using RGD-derivatized

PEGDM hydrogels possessing a continuous Young's modulus gradient. Acta Biomater. 2013; 9:6095–104. [PubMed: 23291491]

57. Jeschke B, Meyer J, Jonczyk A, Kessler H, Adamietz P, Meenen NM, et al. RGD-peptides for tissue engineering of articular cartilage. Biomaterials. 2002; 23:3455–63. [PubMed: 12099289]
58. Kilian KA, Bugarija B, Lahn BT, Mrksich M. Geometric cues for directing the differentiation of mesenchymal stem cells. Proc Natl Acad Sci. 2010; 107:4872–7. [PubMed: 20194780]
59. Treiser MD, Yang EH, Gordonov S, Cohen DM, Androulakis IP, Kohn J, et al. Cytoskeleton-based forecasting of stem cell lineage fates. Proc Natl Acad Sci. 2010; 107:610–5. [PubMed: 20080726]
60. Benya PD, Padilla SR. Dihydrocytochalasin B enhances transforming growth factor-[beta]-induced reexpression of the differentiated chondrocyte phenotype without stimulation of collagen synthesis. Exp Cell Res. 1993; 204:268–77. [PubMed: 8440324]
61. Benya PD, Brown PD, Padilla SR. Microfilament modification by dihydrocytochalasin B causes retinoic acid-modulated chondrocytes to reexpress the differentiated collagen phenotype without a change in shape. J Cell Biol. 1988; 106:161–70. [PubMed: 3276711]
62. Brown PD, Benya PD. Alterations in chondrocyte cytoskeletal architecture during phenotypic modulation by retinoic acid and dihydrocytochalasin B-induced reexpression. J Cell Biol. 1988; 106:171–9. [PubMed: 3276712]
63. Place ES, Evans ND, Stevens MM. Complexity in biomaterials for tissue engineering. Nat Mater. 2009; 8:457–70. [PubMed: 19458646]
64. Engler AJ, Sen S, Sweeney HL, Discher DE. Matrix elasticity directs stem cell lineage specification. Cell. 2006; 126:677–89. [PubMed: 16923388]
65. Engler A, Bacakova L, Newman C, Hategan A, Griffin M, Discher D. Substrate compliance versus ligand density in cell on gel responses. Biophys J. 2004; 86:617–28. [PubMed: 14695306]
66. Zustiak SP, Durbal R, Leach JB. Influence of cell-adhesive peptide ligands on poly(ethylene glycol) hydrogel physical, mechanical and transport properties. Acta Biomater. 2010; 6:3404–14. [PubMed: 20385260]
67. Bryant SJ, Anseth KS. Hydrogel properties influence ECM production by chondrocytes photoencapsulated in poly(ethylene glycol) hydrogels. J Biomed Mater Res. 2002; 59:63–72. [PubMed: 11745538]
68. Klein TJ, Rizzi SC, Schrobback K, Reichert JC, Jeon JE, Crawford RW, et al. Long-term effects of hydrogel properties on human chondrocyte behavior. Soft Matter. 2010; 6:5175–83.
69. Roberts JJ, Earnshaw A, Ferguson VL, Bryant SJ. Comparative study of the viscoelastic mechanical behavior of agarose and poly(ethylene glycol) hydrogels. J Biomed Mater Res B Appl Biomater. 2011; 99B:158–69. [PubMed: 21714081]
70. Murray DH, Bush PG, Brenkel IJ, Hall AC. Abnormal human chondrocyte morphology is related to increased levels of cell-associated IL-1β and disruption to pericellular collagen type VI. J Orthop Res. 2010; 28:1507–14. [PubMed: 20872589]
71. Daniels K, Solursh M. Modulation of chondrogenesis by the cytoskeleton and extracellular matrix. J Cell Sci. 1991; 100:249–54. [PubMed: 1757484]
72. Nofal GA, Knudson CB. Latrunculin and cytochalasin decrease chondrocyte matrix retention. J Histochem Cytochem. 2002; 50:1313–23. [PubMed: 12364564]
73. Fioravanti A, Nerucci F, Annefeld M, Collodel G, Marcolongo R. Morphological and cytoskeletal aspects of cultivated normal and osteoarthritic human articular chondrocytes after cyclical pressure: a pilot study. Clin Exp Rheumatol. 2003; 21:739–46. [PubMed: 14740453]
74. Koshimizu T, Kawai M, Kondou H, Tachikawa K, Sakai N, Ozono K, et al. Vinculin functions as regulator of chondrogenesis. J Biol Chem. 2012; 287:15760–75. [PubMed: 22416133]

Appendix A. Figures with essential colour discrimination

Certain figures in this article, particularly Figs. 1, 4 and 5, are difficult to interpret in black and white. The full colour images can be found in the on-line version, at http://dx.doi.org/10.1016/j.actbio.2013.04.005.

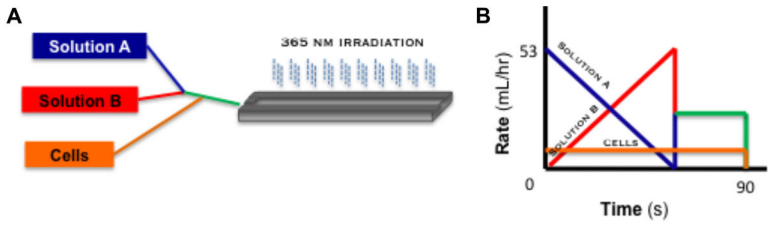

Fig. 1.

Illustration of computer driven syringe pump system for the RGD concentration gradient fabrication. (A) Schematic of the gradient fabrication system, pumping of solutions A, B and cells into the mold followed by irradiation at 465 nm for 5 min. (B) Depiction of the computer controlled pumping program, inverse ramp rates for solutions A (11.5% PEGDM ~8000 g mol^{-1}) and B (11.5% PEGDM ~8000 g mol^{-1}, w/15 mM acrylated RGD) from 0 ml h^{-1} to 53 ml h^{-1} and the chondrocytes at a constant rate for 90 s. Both solutions were prepared containing 0.1% Irgacure 2959 as an initiating system.

A

Characterization Modality	Average Value ± Standard Deviation
Young's Modulus	1950 Pa ± 460 Pa
Shear Modulus	95.4 kPa ± 23.1 kPa
Storage Modulus	4810 Pa ± 260 Pa
Loss Modulus	43.1 Pa ± 11.3 Pa
Swelling Ratio	13 ± 2
Water Content	92 % ± 1 %
Mesh Size	119 Å ± 10 Å

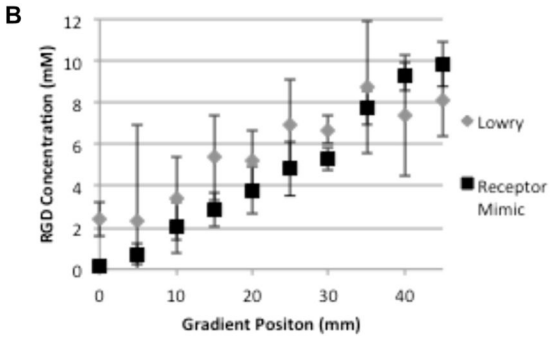

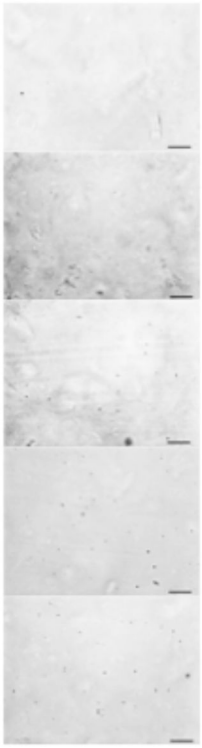

Fig. 2.

Hydrogel characterization. (A) Mechanical properties including storage modulus, loss modulus, swelling ratio, water content and mesh size of the hydrogel. (B) Quantification of RGD concentration every 5 mm along the length of the hydrogel using the Lowry assay and our integrin mimicking gold nanoparticle labeling. (C) Bright-field microscopy images showing bioavailable RGD-labeled with gold nanoparticles (black dots) at 10 mm intervals. Scale bar = 50 μm.

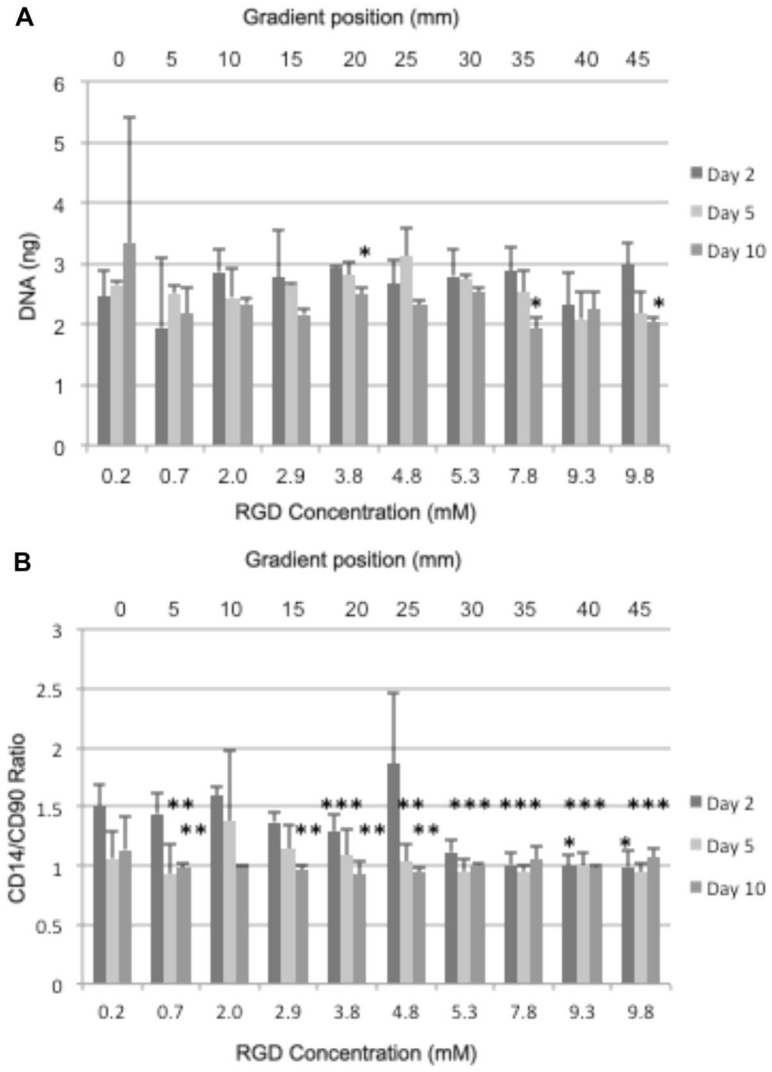

Fig. 3.

Chondrocyte survival of each gradient position based on DNA (ng) for days 2, 5, and 10 (A) and phenotype maintenance using CD14/CD90 ratios for days 2, 5, and 10 (B). 10 days of culture. $^{*}P$-value < 0.05 relative to the 2.4 mM RGD concentration (10 mm gradient position). $^{**}P$-value < 0.05 relative to the 2 day value. $^{***}P$-value < 0.05 relative to the 4.8 mM RGD concentration (25 mm gradient position).

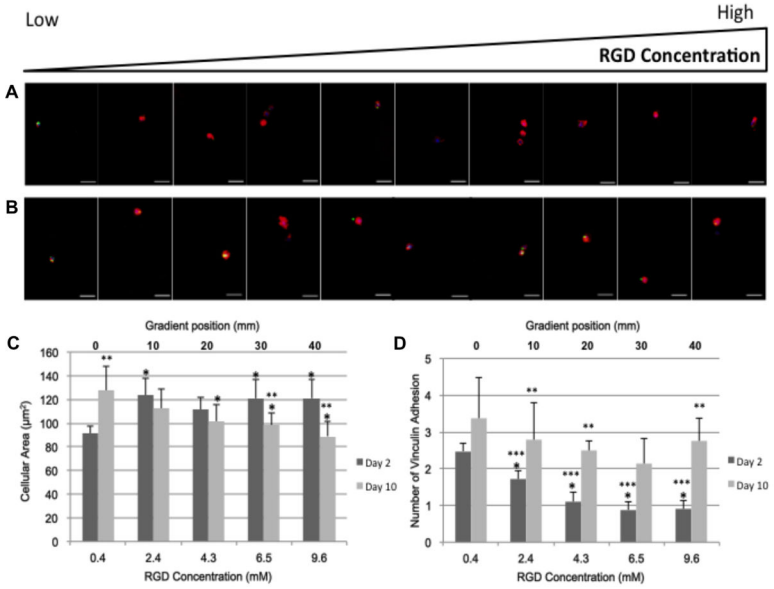

Fig. 4.

Actin (red), vinculin (green) and nuclear (blue) staining after (A) 2 days and (B) 10 days of culture. Images where taken every 5 mm down the length of the gradient. Scale bar = 25 μm. Quantification of (C) cellular area (μm^2) for days 2 and 10 and (D) the number of vinculin adhesions for days 2 and 10 per cell. $^{*}P$-value < 0.05 relative to the 0.4 mM RGD concentration (0 mm gradient position). $^{**}P$-value < 0.05 relative to the 2 day value for the gradient position. $^{***}P$-value < 0.05 relative to the 2.4 mM RGD concentration (10 mm gradient position).

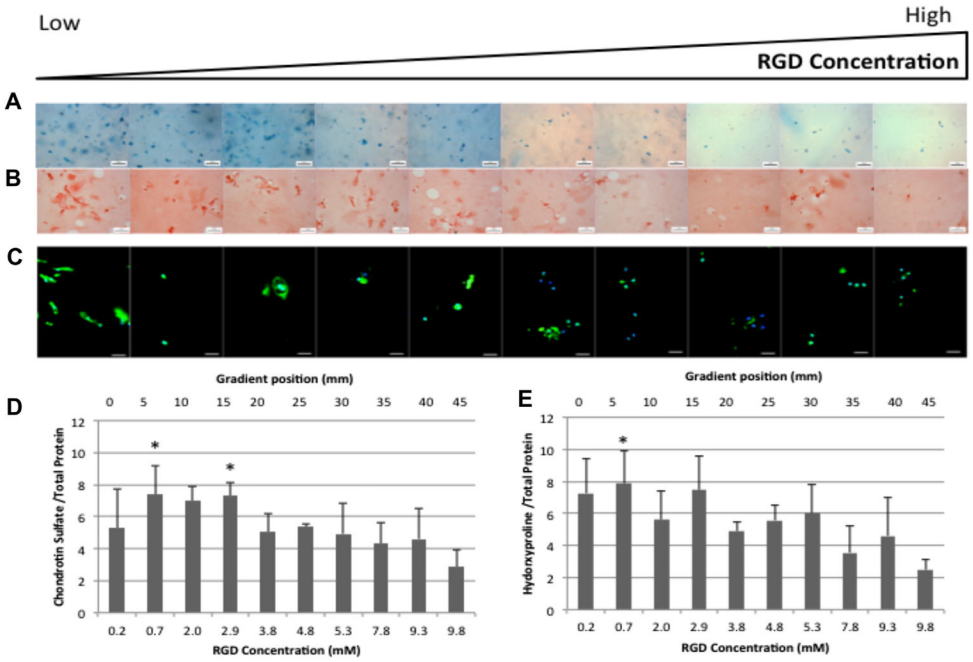

Fig. 5.

Extracellular matrix production by human chondrocytes after 3 weeks of culture. Images where taken every 5 mm down the length of the gradient. (A) Whole mount Alcian Blue staining. Scale bar = 200 μm. (B) Sirius red staining of histological sections. Scale bar = 50 μm. (C) Type 2 collagen (green) and nuclear (blue) immunofluorescence of histological sections. Scale bar = 25 μm. (D) Sulfated gylcosaminoglycan biochemical quantification for week 3. (E) Hydroxyproline biochemical quantification for week 3. $^{*}P$-value ≤ 0.05 relative to the 9.8 mM RGD concentration (45 mm gradient position).